Research article JHEP|Reports

Increased sinusoidal pressure impairs liver endothelial mechanosensing, uncovering novel biomarkers of portal hypertension

Authors

Martí Ortega-Ribera, **Albert Gibert-Ramos**, Laia Abad-Jordà, Marta Magaz, Luis Téllez, Lorena Paule, Elisa Castillo, Raül Pastó, Bruno de Souza Basso, Pol Olivas, Lara Orts, Juan José Lozano, Rosa Villa, Jaime Bosch, Agustín Albillos, Joan Carles García-Pagán, Jordi Gracia-Sancho

Correspondence

jgracia@recerca.clinic.cat (J. Gracia-Sancho).

Graphical abstract

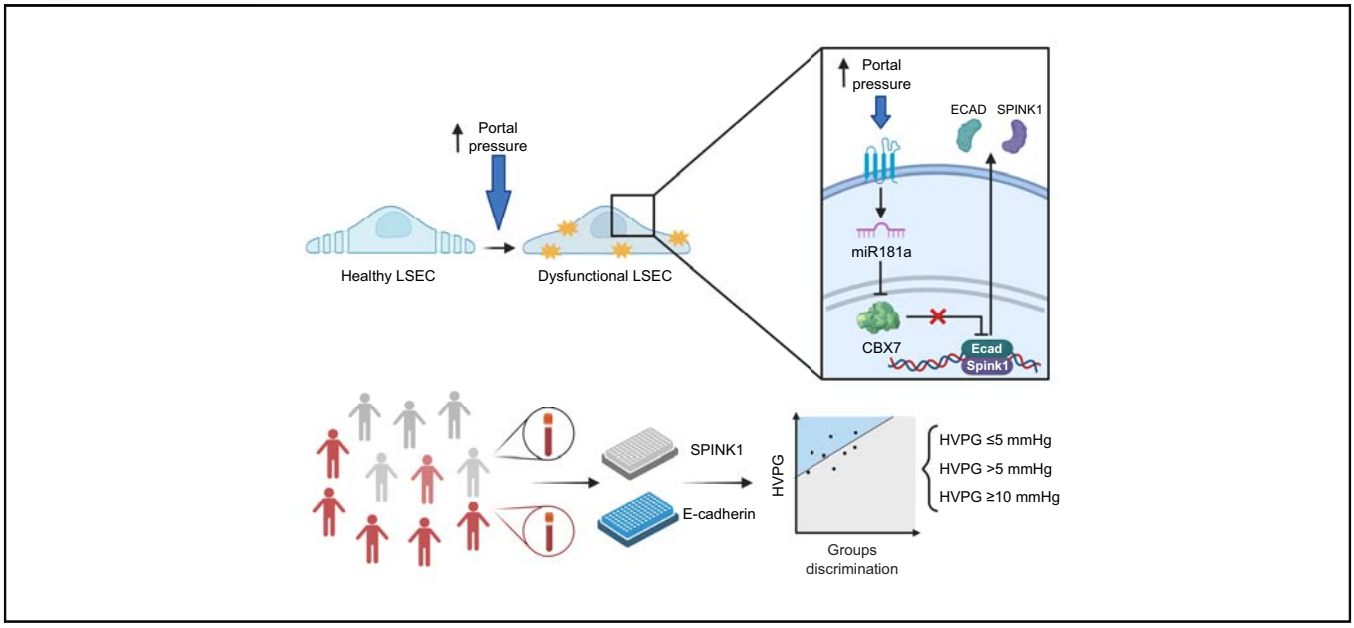

Highlights

- Using a microfluidic liver-on-a-chip device, we showed that pathological pressure is deleterious on LSEC phenotype.
- RNAseq identified CBX7 as a key transcription factor in LSEC downregulated by pathological pressure.
- Hepatic CBX7 downregulation by pressure was validated in patients with portal hypertension and correlated with HVPG.
- MiR-181a-5p was identified as a pressure-induced upstream regulator of CBX7.
- ECAD and SPINK1, targets of CBX7, were predictive of portal hypertension and clinically significant portal hypertension.

Impact and Implications

Increased pressure in the portal venous system that typically occurs during chronic liver disease (called portal hypertension) is one of the main drivers of related clinical complications, which are linked to a higher risk of death. In this study, we found that pathological pressure has a harmful effect on liver sinusoidal endothelial cells and identified CBX7 as a key protein involved in this process. CBX7 regulates the expression of E-cadherin and SPINK1, and consequently, measuring these proteins in the blood of patients with chronic liver disease allows the prediction of portal hypertension and clinically significant portal hypertension.

https://doi.org/10.1016/j.jhepr.2023.100722

Research article

JHEP|Reports

Increased sinusoidal pressure impairs liver endothelial mechanosensing, uncovering novel biomarkers of portal hypertension

Martí Ortega-Ribera,[1,†] **Albert Gibert-Ramos**,[1,†] Laia Abad-Jordà,[1,2] Marta Magaz,[1,2] Luis Téllez,[2,3] Lorena Paule,[2,3] Elisa Castillo,[3] Raül Pastó,[1] Bruno de Souza Basso,[1,4] Pol Olivas,[1] Lara Orts,[1,2] Juan José Lozano,[2] Rosa Villa,[5,6] Jaime Bosch,[1,2,7] Agustín Albillos,[2,3] Joan Carles García-Pagán,[1,2] Jordi Gracia-Sancho[1,2,7,*]

[1]*Liver Vascular Biology Research Group, Barcelona Hepatic Hemodynamic Laboratory, IDIBAPS Biomedical Research Institute, Barcelona, Spain;* [2]*Biomedical Research Networking Center in Hepatic and Digestive Diseases (CIBEREHD), Madrid, Spain;* [3]*Gastroenterology and Hepatology Department, Hospital Universitario Ramon y Cajal, Instituto Ramon y Cajal de Investigacion Biosanitaria (IRYCIS), Universidad de Alcalá, Madrid, Spain;* [4]*PUCRS, Escola de Ciências, Laboratório de Pesquisa em Biofísica Celular e Inflamação, Porto Alegre, Brazil;* [5]*Grupo de Aplicaciones Biomédicas, Institut de Microelectrònica de Barcelona, IMB-CNM (CSIC), Esfera UAB, Bellaterra, Spain;* [6]*Biomedical Research Networking Center in Bioengineering, Biomaterials and Nanomedicine (CIBERBBN), Madrid, Spain;* [7]*Department of Visceral Surgery and Medicine, Inselspital, Bern University Hospital, University of Bern, Bern, Switzerland*

JHEP Reports **2023.** https://doi.org/10.1016/j.jhepr.2023.100722

Background & Aims: Portal hypertension (PH) is a frequent and severe clinical syndrome associated with chronic liver disease. Considering the mechanobiological effects of hydrostatic pressure and shear stress on endothelial cells, we hypothesised that PH might influence the phenotype of liver sinusoidal endothelial cells (LSECs) during disease progression. The aim of this study was to investigate the effects of increased hydrodynamic pressure on LSECs and to identify endothelial-derived biomarkers of PH.

Methods: Primary LSECs were cultured under normal or increased hydrodynamic pressure within a pathophysiological range (1 *vs*. 12 mmHg) using a microfluidic liver-on-a-chip device. RNA sequencing was used to identify pressure-sensitive genes, which were validated in liver biopsies from two independent cohorts of patients with chronic liver disease with PH (n = 73) and participants without PH (n = 23). Biomarker discovery was performed in two additional independent cohorts of 104 patients with PH and 18 patients without PH.

Results: Transcriptomic analysis revealed marked deleterious effect of pathological pressure in LSECs and identified chromobox 7 (*CBX7*) as a key transcription factor diminished by pressure. Hepatic *CBX7* downregulation was validated in patients with PH and significantly correlated with hepatic venous pressure gradient. MicroRNA 181a-5p was identified as pressure-induced upstream regulator of CBX7. Two downstream targets inhibited by CBX7, namely, E-cadherin (ECAD) and serine protease inhibitor Kazal-type 1 (SPINK1), were found increased in the bloodstream of patients with PH and were highly predictive of PH and clinically significant PH.

Conclusions: We characterise the detrimental effects of increased hydrodynamic pressure on the sinusoidal endothelium, identify CBX7 as a pressure-sensitive transcription factor, and propose the combination of two of its reported products as biomarkers of PH.

Impact and Implications: Increased pressure in the portal venous system that typically occurs during chronic liver disease (called portal hypertension) is one of the main drivers of related clinical complications, which are linked to a higher risk of death. In this study, we found that pathological pressure has a harmful effect on liver sinusoidal endothelial cells and identified CBX7 as a key protein involved in this process. CBX7 regulates the expression of E-cadherin and SPINK1, and consequently, measuring these proteins in the blood of patients with chronic liver disease allows the prediction of portal hypertension and clinically significant portal hypertension.

© 2023 The Author(s). Published by Elsevier B.V. on behalf of European Association for the Study of the Liver (EASL). This is an open access article under the CC BY-NC-ND license (http://creativecommons.org/licenses/by-nc-nd/4.0/).

Keywords: Liver sinusoidal endothelial cells; LSEC; Hepatic haemodynamic; Liver cirrhosis; HVPG; Endothelial dysfunction; Mechanotransduction; Mechanobiology; NASH; HCV.

Received 12 July 2022; received in revised form 24 February 2023; accepted 27 February 2023; available online 8 March 2023

† These authors share co-first authorship.

* Corresponding author. Address: IDIBAPS Biomedical Research Institute, Rosselló 149, 08036, Barcelona, Spain. Tel.: +34 932275400 #4306

E-mail address: jgracia@recerca.clinic.cat (J. Gracia-Sancho).

Introduction

Advanced chronic liver disease (ACLD) is nowadays the 11th most common cause of death globally with approximately 1.16 million deaths per year.[1,2] Alcohol abuse, chronic viral hepatitis B or C infection, and metabolic-associated fatty liver disease are amongst the most frequent causes of this condition. Portal hypertension (PH) is one of the main drivers of ACLD-related clinical

complications including bleeding from gastro-oesophageal varices, ascites, or hepatic encephalopathy,[3,4] and predisposes the patient with cirrhosis to acute-on-chronic liver failure.[5,6]

The primary factor in the development of PH is a marked increase in the intrahepatic vascular resistance to portal blood flow, which occurs during the progression of fibrosis as a consequence of sinusoidal cell deregulation.[7] During persistent liver injury, liver sinusoidal endothelial cells (LSECs) become dysfunctional, losing their characteristic transmembrane pores named as fenestrae and increasing basement lamina deposition,[8,9] a process known as sinusoidal capillarisation. Capillarisation impairs the exchange of blood-borne molecules with neighbouring cells and contributes to hepatocyte dedifferentiation and death.[9–11] During liver injury, hepatic stellate cells (HSCs) activate and differentiate into extracellular matrix-secreting myofibroblasts, whereas Kupffer cells (KCs) polarise towards a pro-inflammatory phenotype recruiting monocytes to the site of injury for tissue repair.[12,13] Both microvascular dysfunction and fibrotic architectural distortion, imbalance of vasoactive mediators, and microthrombi formation leads to altered mechanical properties of the tissue, further increasing the vascular resistance and, ultimately, elevating the sinusoidal pressure. Despite the fact that LSECs, owing to their particular sinusoidal location, are the first cells sensing changes in intravascular pressure, the possible direct contribution of this mechanobiological cue to LSEC dysfunctionality in the ACLD setting remains largely unknown.

Currently, hepatic venous pressure gradient (HVPG) is the most reliable method for diagnosing cirrhotic PH and allows stratification of patients with normal pressure (NP, HVPG ≤5 mmHg), PH (HVPG >5 mmHg), and clinically significant PH (CSPH, HVPG ≥10 mmHg). Patients with CSPH are at risk of developing clinical complications and are thus at increased risk of hepatic decompensation and death.[14,15] However, HVPG measurement is an invasive procedure with limitations including availability, affordability, and requiring specifically trained personnel.[16,17] The unmet clinical need of easy and reliable non-invasive tests for PH monitoring[18] prompted us to explore LSEC-derived pressure-associated biomarkers for PH and CSPH in patients with ACLD. According to our hypothesis, as LSECs are directly in contact with blood flow, factors specifically secreted by this cell type in response to changes in portosinusoidal pressure might be detectable in the systemic bloodstream, being therefore potentially useful as non-invasive biomarkers.

Overall, the present study aimed at investigating the influence of pathological hydrodynamic pressure *per se* in LSECs function and to discover pressure-sensitive biomarkers that could be used for non-invasive assessment of PH in clinical practice.

Materials and methods

Animals

Male Wistar rats were kept at the University of Barcelona Faculty of Medicine facilities, housed three per cage, under controlled environmental conditions (19.7 ± 2 °C, 52 ± 5% humidity, 12-h light/dark cycle) and free access to standard rodent food pellets and water. All the experimental procedures were approved by the Laboratory Animal Care and Use Committee of the University of Barcelona and performed in accordance with the European Community guidelines for the protection of animals used for experimental and other scientific purposes (EEC Directive 86/609).

Isolation of hepatic cells

Primary hepatocytes and non-parenchymal cells from healthy rats weighing 300–350 g and carbon tetrachloride (CCl_4)-induced cirrhotic rats[19] were isolated using the '4 in 1' protocol as previously reported.[20] Briefly, liver was perfused, digested with 0.015% collagenase A (103586, Roche, Sant Cugat del Vallès, Spain), and mechanically disaggregated, obtaining a multicellular suspension. Hepatocytes were purified by low-speed centrifugation, and non-parenchymal cells were separated using a three-phase iodixanol (Optiprep™, Sigma-Aldrich, Saint Louis, MO, USA) density gradient centrifugation. Subsequently, the upper interphase, which contained the HSCs, was directly seeded, whereas the lower one, enriched in LSECs and KCs, was further purified by differential adherence time to non-coated substrates. Highly pure (>95%) and viable (80–95%) cells[20] were seeded at high density on conventional culture plates or on liver-on-a-chip devices.

Hydrodynamic pressure on a liver-on-a-chip device

The study of hydrodynamic pressure *in vitro* was performed using an advanced sinusoid-mimicking microfluidic device (Exoliver, Barcelona Liver Bioservices, Barcelona, Spain; Fig. S1). The details of its fabrication, features, and suitability for sinusoidal studies have been previously reported.[19,21] Primary cells isolated from healthy rats were exposed to physiological (1 mmHg) or pathological (12 mmHg) pressures within the liver-on-chip device for 48 h. The laminar shear stress stimulus on LSEC cultures was maintained at 1.15 dynes/cm^2 to preserve their functionality during long-term culture, as previously described.[21]

The desired hydrodynamic pressure within the device was ensured by modulating outflow height relative to LSEC culture and according to 1 mmHg = 1.36 cm H_2O. Real-time assessment of pressure within the bioreactor was routinely performed in independent experimental settings with a constant flow of 1.5 ml/min and using a pressure probe at both the inflow and outflow of the device connected to a Powerlab (4SP, ADInstruments, Castle Hill, NSW, Australia). Data were displayed into a LabChart v5.5.6 (ADInstruments) software file.

Device configuration and culture was performed as previously described.[21] LSECs were cultured on a hydrophilic biocompatible polytetrafluoroethylene microporous membrane, and hepatocytes, KCs, and HSCs at a lower layer, in contact with the endothelial fraction of the culture. Microfluidic cultures were maintained at 37 °C and 5% CO_2, with 43 ml of recirculating media as follows: DMEM F12® was supplemented with 2.97% dextran (31392; Sigma-Aldrich, Darmstadt, Germany), 2% FBS (04-001-1A; Biological Industries, Kibbutz Beit-Haemek, Israel), 1% penicillin–streptomycin (10378-016, Biological Industries), 1% endothelial cell growth supplement (BT-203; Biomedical Technologies, Kandel, Germany), 1% heparin (H3393; Sigma-Aldrich), 1% L-glutamine (25030-024; Gibco, Dublin, Ireland), 1% amphotericin B (03-029-1C; Biological Industries), 1 nM dexamethasone (D4902; Sigma-Aldrich), 10 ng/ml Epidermal Growth Factor (E4127; Sigma-Aldrich), 1.5 nM glucagon (16941-32-4, Novo Nordisk, Plainsboro, NJ, USA), 15 nM hydrocortisone (H0888, Sigma-Aldrich), and 1 μM insulin (Humulin S, Lilly S.A, Alcobendas, Madrid, Spain).

mRNA sequencing

Primary LSECs transcriptome profile under physiological or increased hydrodynamic pressures was examined by mRNA sequencing from three independent experiments. Briefly, mRNA was isolated using the RNeasy® Micro Kit (Qiagen, Hilden,

Germany) following the manufacturer's instructions. The sequencing library was prepared using 25 ng of total RNA by a Universal Plus mRNA-Seq NuGEN (0508, 9133, 9134, Tekan, Leek, The Netherlands). Single-end mRNA sequencing was performed in the Illumina platform HiSeq2500 (Illumina Inc, San Diego, California, U.S.). The dataset is available at the National Center for Biotechnology Information Gene Expression Omnibus database, accession number GSE181255. Genes were considered significantly deregulated when their fold change was >3 or <-3 and their *p* value <0.05. Venn diagrams were created using the Venny2.1 free online software (by Juan Carlos Oliveros, BioinfoGP, CNB–CSIC). Human and murine genes were compared by homology (~90% rat genes have an orthologue in the human genome). Canonical pathway analysis was performed using the Ingenuity Pathways Analysis software from Qiagen (content version 49932394). Transcriptomics data from LSECs isolated from preclinical models of ACLD (CCl_4, thioacetamide [TAA], and common bile duct ligation [cBDL]) and patients with alcohol-associated cirrhosis were obtained from a previous publication from our group.[22]

miR-181-5p inhibition

Primary rat LSECs were cultured on a 12-well plate at 80–90% confluency. Two hours after the isolation, cells were transfected with Lipofectamine RNAiMAX Transfection Reagent (13778075, Thermo Fisher, Waltham, MA, USA) containing 50 nM mirVana™ micro RNA (miRNA) inhibitor hsa-miR-181a-5p or scramble construct for 48 h following the manufacturer's instructions.

For miR-181a-5p expression analyses, Qiazol Lysis Reagent and the miRNeasy® Micro Kit (Qiagen) were used for total RNA preservation and purification. miR-181a-5p expression was assessed by using TaqMan MicroRNA Assays (Applied Biosystems, Madrid, Spain) with TaqMan Universal Master Mix II, no UNG (Applied Biosystems). Data were normalised to U6 snRNA expression.

Gene expression analysis

Total RNA was extracted and purified with TRItidy G™ (A4051,0200, Panreac, Castellar del Vallès, Spain) and TRIzol:-chloroform for liver tissues or using Qiazol Lysis Reagent and the RNeasy® Micro Kit (Qiagen) for primary cells according to the manufacturer's instructions. RNA yield was quantified using a Nanodrop ND-1000 spectrophotometer (NanoDrop Technologies, Wilmington, DE, USA). A total amount of 0.5 μg (tissue) and 0.15 μg (cells) RNA was reverse transcribed using a High-Capacity cDNA Reverse Transcription Kit (Applied Biosystems) in a thermal cycler (Eppendorf AG 22331, Hamburg, Germany), and quantitative PCR was performed in a 7900HT Fast Real-Time PCR System (Thermo Fisher), using the TaqMan Universal PCR Master Mix (Applied Biosystems).

RNA expression levels were normalised following the $2^{-\Delta\Delta Ct}$ method, with beta actin (Actb) or glyceraldehyde-3-phosphate dehydrogenase (Gapdh) as housekeeping genes. The following TaqMan probes were used: chromobox 7 (*CBX7*, Rn01506264_m1 and Hs00545603_m1), Fc-gamma receptor IIb (*CD32b*, Rn00598391 m1), stabilin 2 (*Stab2*, Rn01503539_m1), *Actb* (Hs99999903_m1), *Gapdh* (Rn01775763_g1), hsa-miR-181a-5p (000480), and U6 snRNA (001973).

Scanning electron microscopy imaging

Primary rat LSECs were cultured on a circular coverglass with 18 mm of diameter and fixed overnight with 2% glutaraldehyde dissolved in 0.1M cacodylate buffer (pH 7.4). Cells were washed three times with the cacodylate buffer for 5 min and incubated for 1 h with 1% tannic acid and 2 h with 2% osmic acid. Subsequently, cells were dehydrated with an ethanol battery (50, 70, 90, 95, and 100%), critical-point dried with carbon dioxide, sputter coated with gold, and examined by scanning electron microscopy.[20]

Patients

Four different cohorts of patients from the Hospital Clinic of Barcelona and the Ramon y Cajal Hospital Madrid (Spain) were included in this study:

- Discovery and validation cohorts. These two cohorts included patients that had HVPG measurement during a transjugular liver biopsy procedure using an 18-G Tru-cut needle that yielded a 20-mm-length liver biopsy. Correlation between HVPG and tissue expression of pressure-sensitive candidate genes was first assessed in a retrospective discovery cohort and further validated in a larger cohort (validation cohort). The discovery cohort consisted of 12 patients without PH and 19 patients with PH with cirrhosis caused by chronic HCV infection. The validation cohort was prospectively collected and comprised 11 patients without PH, 40 patients with PH with cirrhosis caused by HCV (n = 16) and alcohol (OH, n = 24) aetiologies, and 14 patients with HCV cirrhosis with sustained virological response (12 months after finalising antiviral treatment). Patients without portal hypertension had biopsy and HVPG procedures owing to previous suspicion of PH that was not confirmed and that had no signs of significant liver disease on liver biopsy examination.
- Discovery and validation biomarker cohorts. These cohorts included patients having HVPG measurements and a peripheral blood sample collected just before HVPG measurements and were used to discover and independently validate pressure-related non-invasive biomarkers for PH. The discovery biomarker cohort was a prospective one with 18 patients with NP and 47 patients with chronic liver disease (CLD)-derived PH enrolled at the Barcelona Hepatic Hemodynamic Unit. The validation biomarker cohort was external and retrospective, including 57 patients with CLD-derived PH from the Hepatology Unit of the Ramón y Cajal Hospital, Madrid.

Patients included in all cohorts underwent HVPG measurement owing to clinical indications. The protocol of this study was reviewed and approved by the Ethical Committees for Clinical Investigation of the Hospital Clınic of Barcelona and the Ramón y Cajal Hospital and was in accordance with the Helsinki Declaration of 1975, as revised in 1983. Written informed consent was obtained from each patient.

HVPG measurement

HVPG measurement was performed as described.[23] In short, a 7F balloon-tipped catheter (Fogarty®, Edwards Lifesciences LLC, Irvine, CA, USA) was guided into the main right or middle hepatic vein for measurements of wedged and free hepatic venous pressures. The HVPG was calculated as the difference between both measurements. All measurements were taken by triplicate and averaged to obtain the baseline HVPG. Permanent tracings were obtained in each case in a multichannel recorder (GE Healthcare, Milwaukee, WI, USA).

In addition, liver stiffness measurement was performed by transient elastography (FibroScan®; Echosens, Paris, France) together with determination of plasma albumin, bilirubin, international normalised ratio, and presence of decompensation

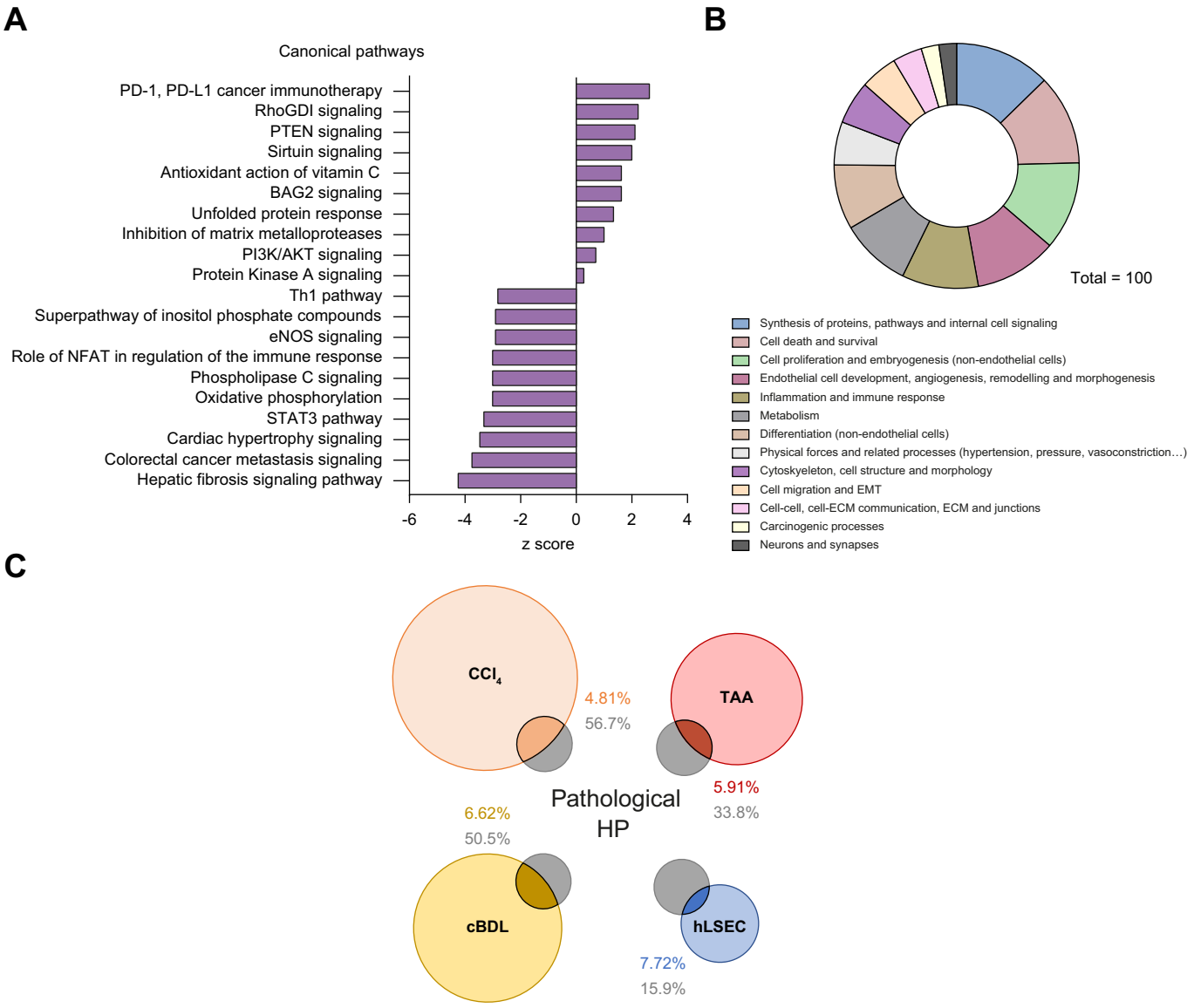

Fig. 1. Effects of pathological pressure in LSECs cultured under pathological hydrodynamic pressure. (A) Top upregulated and downregulated canonical pathways and (B) main molecular processes modified owing to pathological hydrodynamic pressure. (C) Venn diagrams comparing differentially expressed genes from LSECs submitted to pathological pressure (n = 3) and LSECs isolated from three cirrhotic portal hypertension preclinical models and LSECs from human patients with cirrhosis (n = 6). Genes were considered significantly deregulated when their fold change was >3 or <-3 and their *p* value <0.05. cBDL, common bile duct ligation-induced cirrhotic rats; CCl_4, carbon tetrachloride induced-cirrhotic rats; HP, hydrodynamic pressure; hLSEC, LSEC from human patients with cirrhosis; LSEC, liver sinusoidal endothelial cell; TAA, thioacetamide-induced cirrhotic rats.

events for the calculation of the Child–Pugh and model for end-stage liver disease scores.

Plasma collection

For the biomarker cohorts, blood was drawn from patients with ACLD or healthy volunteers, collected in BD Vacutainer® K2 EDTA tubes (KFK286, Becton Dickinson, Franklin Lakes, NJ, USA), immediately kept at 4 °C, centrifuged at 1,300 × *g* for 10 min at 4 °C to obtain the plasma, and further centrifuged at 3,000 × *g* for 15 min at 4 °C to remove contaminating platelets. Plasma was aliquoted and stored in the biobank of IDIBAPS or Ramon y Cajal Hospital at -80 °C following the internal agreement policy until use.

Enzyme linked immunosorbent assay

Levels of E-cadherin (ECAD) and serine protease inhibitor Kazal-type 1 (SPINK1) in plasma was measured by ELISA following the manufacturer's instructions. ECAD (ab233611) kits were purchased from Abcam (Cambridge, UK), and SPINK1 (DY7496-05) kits were purchased from R&D Systems (Abingdon, UK).

Statistical analyses

Data are presented as mean ± SD. Sample size for each experiment was evaluated according to previous and exploratory results. Statistical analysis was performed. The normal distribution of the data was evaluated using the Shapiro–Wilk test, with normality assumed for *p* values greater than 0.05. One-way

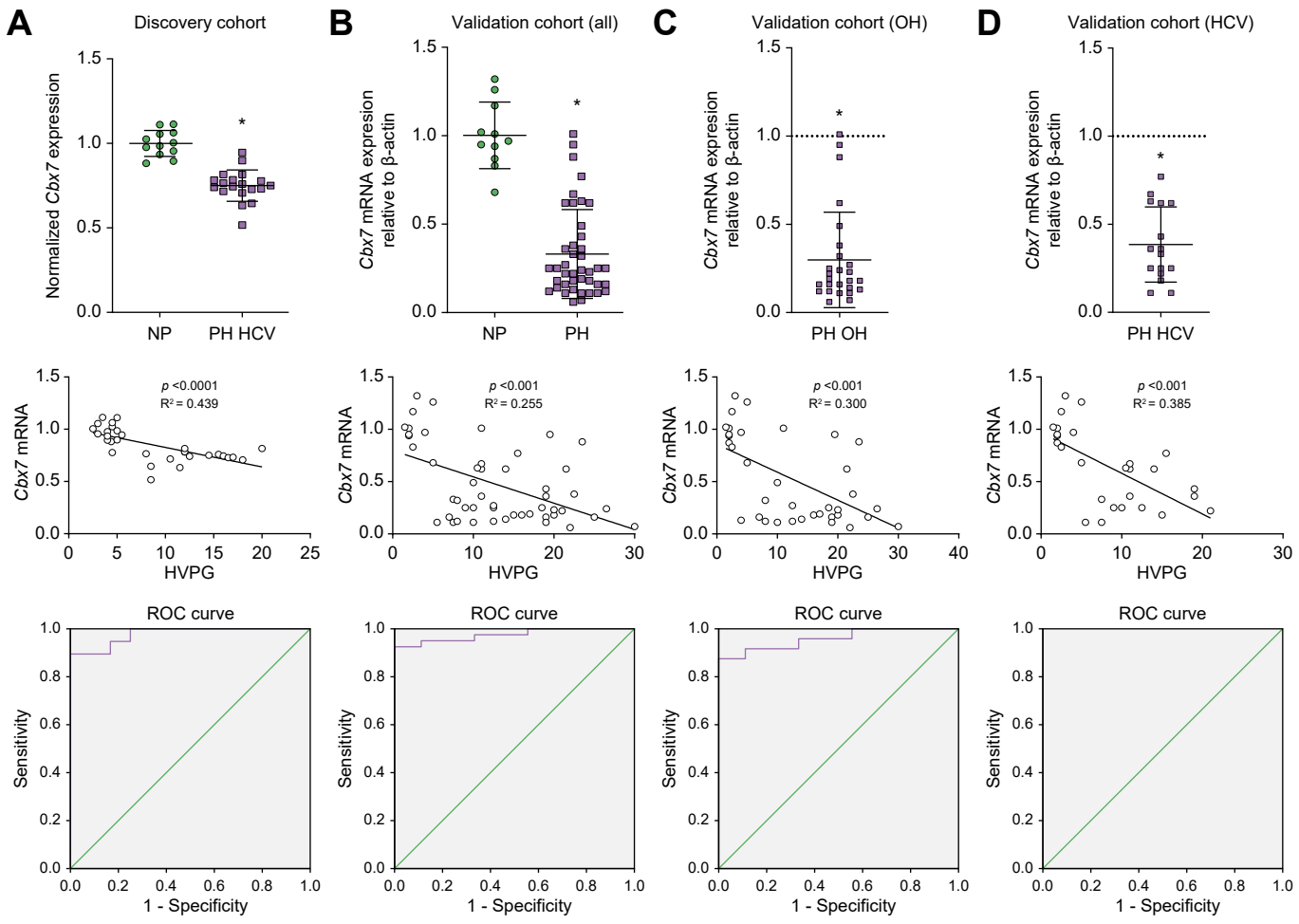

Fig. 2. Hepatic *CBX7* gene expression and correlation with HVPG. Hepatic *CBX7* gene expression (top), its correlation with HVPG (middle), and ROC curves (bottom) in the discovery and validation cohorts. (A) The discovery cohort included patients with NP (NP; n = 12) and patients with PH with HCV-associated CLD (PH HCV; n = 13). (B) The validation cohort included healthy individuals with NP (NP; n = 11) and patients with PH (PH; n = 30). The validation cohort is further split in (C) patients with alcohol-associated cirrhosis (PH OH; n = 18) and (D) patients with HCV-related cirrhosis (PH HCV; n = 12). *CBX7* gene expression data are presented as the mean ± SD, as the ratios of gene expression relative to beta actin, and expressed as a percentage of the healthy group, set at 1. Data were compared using Student's *t* test (**p* <0.05), and correlations were calculated using Pearson's correlation. CBX7, chromobox 7; CLD, chronic liver disease; HVPG, hepatic venous pressure gradient; NP, normal pressure; PH, portal hypertension; ROC, receiver operating characteristic.

ANOVA or Student's *t* test was used for parametric variables, and the Mann–Whitney *U* test was used for non-parametric variables. The correlations were calculated by Pearson's correlation. Statistical significance was set at a *p* value of <0.05. Areas under the receiver operating characteristics (AUROC) curve and cut-off values for the best specificity and sensitivity were established, and positive predictive value (PPV) and negative predictive value (NPV) were calculated. Statistical analyses were performed using GraphPad Prism v8.0.2 (GraphPad Software, Inc, San Diego, CA, USA) or SPSS (IBM, Chicago, IL, USA) software.

Results

Pathological hydrodynamic pressure induces LSEC dysfunction

To understand the effects of pathological hydrodynamic pressure in LSECs, we performed bulk RNA sequencing on rat primary LSECs cultured under physiological (1 mmHg) or increased pressure (12 mmHg). Transcriptomic analysis revealed 201 deregulated genes (183 downregulated and 18 upregulated) with a fold change ≥3 and *p* value < 0.05 in response to pathological pressure. Canonical pathway analysis showed a marked dysregulation of LSEC phenotype under increased hydrodynamic pressure, evidenced as an upregulation in pathways involved in cancer, matrix metalloproteinases inhibition, and angiogenesis, whereas T-cell activation, endothelial nitric oxide synthase signalling, and antioxidant pathways were significantly downregulated (Fig. 1A). Interestingly, classification of the differentially expressed genes (DEG) in molecular process categories showed alterations in LSEC metabolism, cell death and survival, proliferation, angiogenesis/remodelling, and inflammation (Fig. 1B), further demonstrating a global detrimental impact in LSEC homoeostatic functions. Table S1 shows the top 50 deregulated genes in response to pathological hydrodynamic pressure, which includes known markers of LSEC dysfunction/capillarisation such as *Kdr* or *Dll4*.

As increased pressure is part of the complex and multifactorial pathophysiology of ACLD, we then compared the pressure-specific DEG with those observed in LSECs isolated from three different preclinical models of ACLD: chronic CCl_4, chronic TAA,

A

	Species	FC	*p* value	Groups	n
rno-miR-181a-5p	Rn	1.579	0.005	CCl_4 *vs.* sham	6 *vs.* 6
hsa-miR-181a-5p	Hs	1.691	0.032	AALD *vs.* healthy	6 *vs.* 6

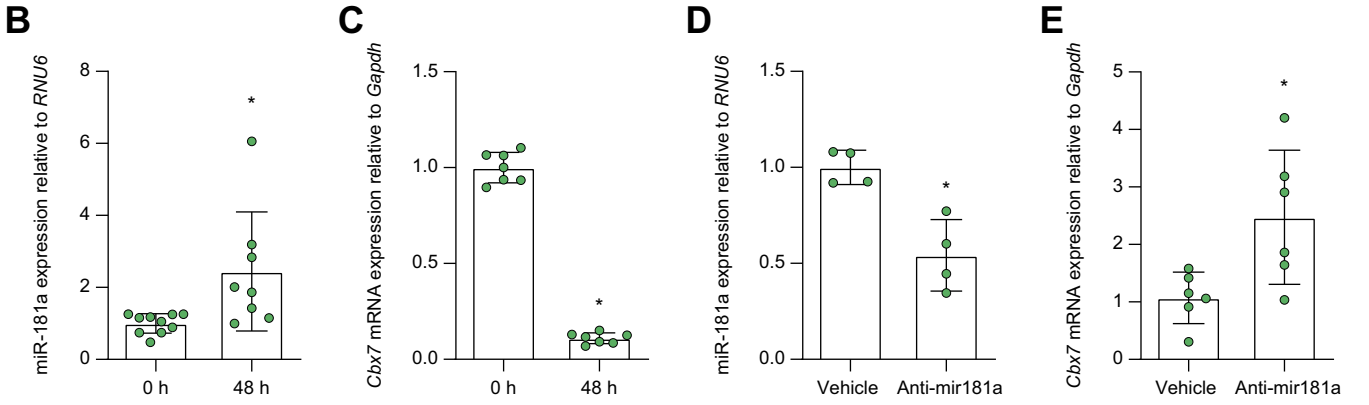

Fig. 3. Expression of miR-181a in LSECs and its effects on *CBX7*. (A) miR-181a-5p expression in cirrhotic LSECs from rat (Rn) and human (Hs), and miR-181a and *CBX7* gene expression in (B and C) LSECs after 48 h of *in vitro* capillarisation and in (D and E) LSECs transfected with an anti-miR-181a. Gene expression data are presented as the mean ± SD, as the ratios of gene expression relative to *RNU6* or *Gapdh* and expressed in comparison with the 0 h group (B and C) or the vehicle group (D and E), set at 1. All experiments were performed with at least n = 4 independent replicates. Data were compared using Student's *t* test (**p* <0.05). AALD, alcohol-associated liver disease; CBX7, chromobox 7; CCl_4, carbon tetrachloride; FC, fold change; GADPH, glyceraldehyde-3-phosphate dehydrogenase; LSEC, liver sinusoidal endothelial cell.

and cBDL. In addition, pressure-specific DEG were also compared with those from primary LSECs isolated from patients with alcohol-associated cirrhosis (human LSECs [hLSECs]). A total of 85% of the DEG found in hLSEC had a known rat orthologue, and interestingly, 70% of the genes detected in hLSEC were also detected in rat LSEC transcriptomic analysis. Comparison between these groups showed that approximately 6% of the cirrhosis-specific DEG were deregulated as well by increased pressure (specifically, DEG deregulated by pressure represented 4.81% for CCl_4, 5.91% for TAA, 6.62% for cBDL, and 7.72% for hLSEC from their total DEG deregulated by cirrhosis) (Fig. 1C), suggesting a contribution of pathological pressure in LSEC dysfunction in ACLD. Conversely, from the total DEG in LSECs exposed to increased hydrodynamic pressure, shared genes represented 56.7% in CCl_4, 33.8% in TAA, 50.5% in cBDL, and 15.9% in hLSEC.

CBX7 is identified as a pressure-related factor in LSECs

We carefully analysed the top 50 DEG list obtained from LSECs cultured under pathological pressure to identify a candidate with potential pleiotropic effects orchestrating LSEC phenotype in response to pressure. *CBX7* appeared as the only gene with transcription regulation activity that was downregulated in LSECs isolated from the three preclinical models of ACLD and in LSECs isolated from patients with cirrhosis (Table S1). Analysis of *CBX7* expression in preclinical models of LSEC capillarisation or in human liver disease from publicly available transcriptomic studies agreed with our findings (Table S2).

Characterisation of *CBX7* abundance in the main liver cell types (hepatocytes, LSECs, HSCs, and KCs) revealed that LSECs are the main cell type expressing this transcription factor in the healthy liver and the only one in which this gene has a downregulated expression in ACLD (Fig. S2).

Hepatic CBX7 downregulation correlates with HVPG in patients with ACLD

To investigate the potential role of *CBX7* as a pressure-sensitive biomarker, we interrogated its gene expression in liver biopsies from two different cohorts of patients with ACLD. The discovery cohort (Table S3) included array expression from patients without PH (n = 12) and patients with HCV cirrhosis with PH (n = 19) with similar age and sex distribution. The majority of patients belonged to Child–Pugh class A. Six patients had an HVPG <10 mmHg, and 13 patients showed an HPVG over 10 mmHg. Liver biopsies from the validation cohort (Table S4) included 40 patients with OH-associated (n = 24) and HCV (n = 16) aetiologies and were analysed by quantitative PCR. Patients' mean age was 58.8 ± 7.5 years for the ACLD group and 56.1 ±16.4 for the non-PH group, both with a similar sex distribution. Child–Pugh scores were evenly distributed, with 15, 16, and 9 patients with scores of A, B, and C, respectively. Regarding HVPG, 7 patients had an HVPG below 10 mmHg, and 33 patients had an HVPG above 10 mmHg.

CBX7 gene expression was analysed in both cohorts, comparing participants without liver disease (HVPG ≤5 mmHg) against patients with PH (HVPG >5 mmHg). *CBX7* was significantly downregulated in patients with PH in both cohorts (Fig. 2A and B, top; *p* <0.0001). *CBX7* downregulation was independent of the aetiology of ACLD (Fig. 2C and 2D, top; *p* <0.0001) and significantly correlated with HVPG (Fig. 2, middle panels). Fig. 2 (bottom panels) shows the receiver operating characteristic (ROC) curves for the discovery and validation cohorts. Of note, these disclosed an excellent diagnostic performance, with an AUROC above 0.964 and with sensitivities of 100% and 92.5% and specificities of 75% and 90.9% for the discovery and validation cohorts, respectively. The performance was independent of aetiology, being similar in patients with HCV and OH (AUROC, 0.994 and 0.943, respectively). Thus, *CBX7* expression was highly

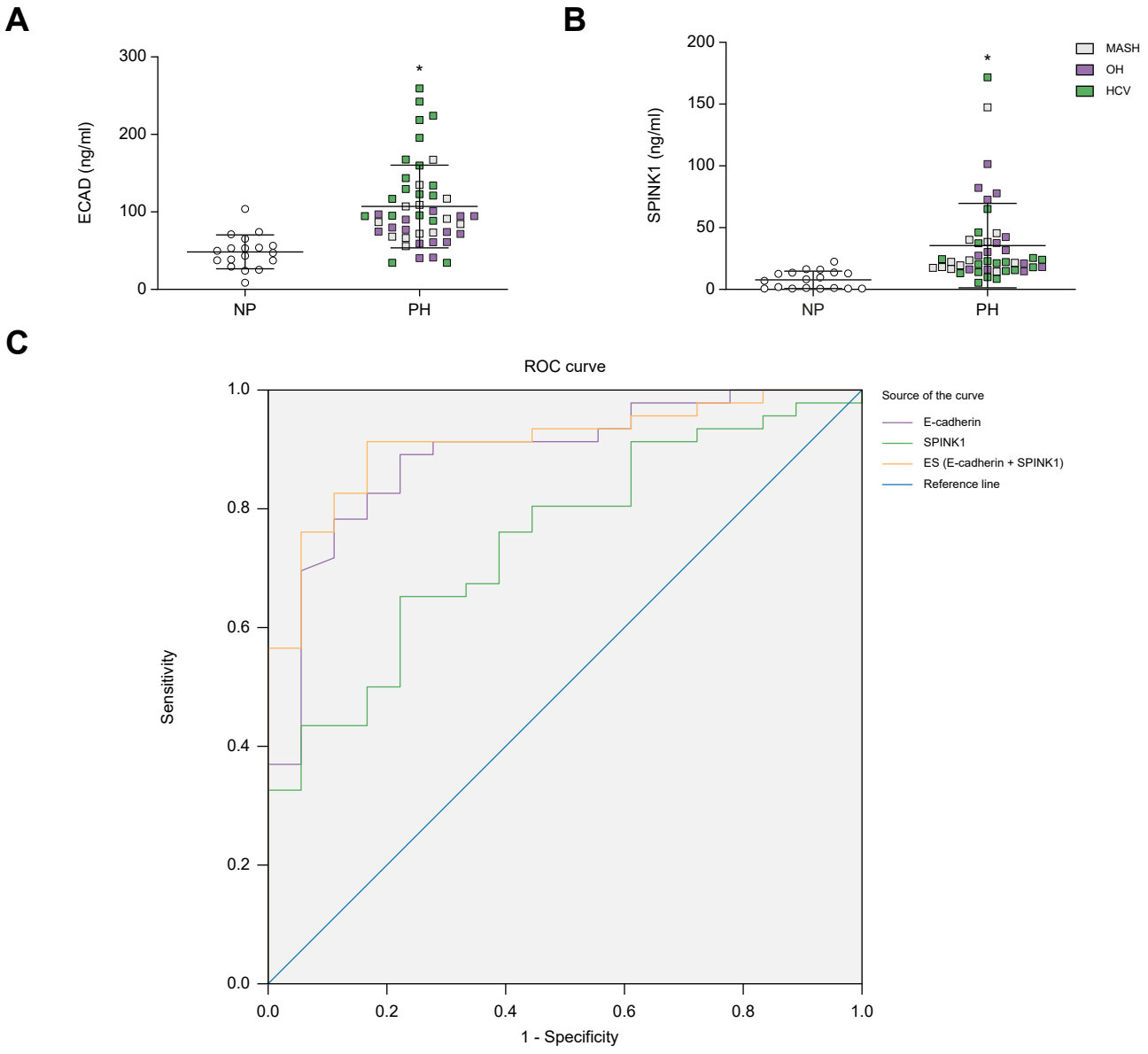

D

Marker	n (</>5 mmHg)	AUROC (95% CI)	Cut-off	Sens (%)	Spec (%)	PPV (%)	NPV (%)
ECAD	18/46	0.889 (0.802 to 0.977)	57.673	89.1	77.8	91.12	73.64
SPINK1	18/45	0.747 (0.622 to 0.871)	16.040	80.0	55.6	81.83	52.65
ECAD + SPINK1	18/45	0.911 (0.838 to 0.983)	0.579	91.3	83.3	93.32	78.93

Fig. 4. Analysis of ECAD, SPINK1, and their combination to predict PH. (A) ECAD and (B) SPINK1 in plasma of healthy humans with NP (NP; n = 18) compared with patients with ACLD with PH (PH; n = 47) of three different aetiologies: MASH, OH, or HCV. (C) ROC curve of ECAD, SPINK1, and ES and (D) its performance. Data were compared using Student's *t* test (*p <0.05). Values of AUROC, the 95% CI, the cut-off value with better Sens and Spec, PPV, and NPV. ACLD, advanced chronic liver disease; AUROC, area under the receiver operating characteristics; ECAD, E-cadherin; ES, ECAD + SPINK1; MASH, metabolic-associated steatohepatitis; NP, normal pressure; NPV, negative predictive value; OH, alcohol-associated; PH, portal hypertension; PPV, positive predictive value; ROC, receiver operating characteristic; Sens, sensitivity; Spec, specificity; SPINK, serine protease inhibitor Kazal-type 1.

sensible, detecting patients with PH. In addition, *CBX7* gene expression was also assessed in a small subgroup of patients with HCV with sustained virological response 12 months after antiviral therapy treatment (Table S4). Interestingly, in these patients, CBX7 was returning towards normal, being significantly higher than that in untreated patients with HCV (+148% *vs*. non-treated patients, p = 0.0134).

Altogether, these results suggest that CBX7 behaves as a pressure-sensitive gene in LSECs, and provide the rationale for further studying the mechanisms regulating *CBX7* expression.

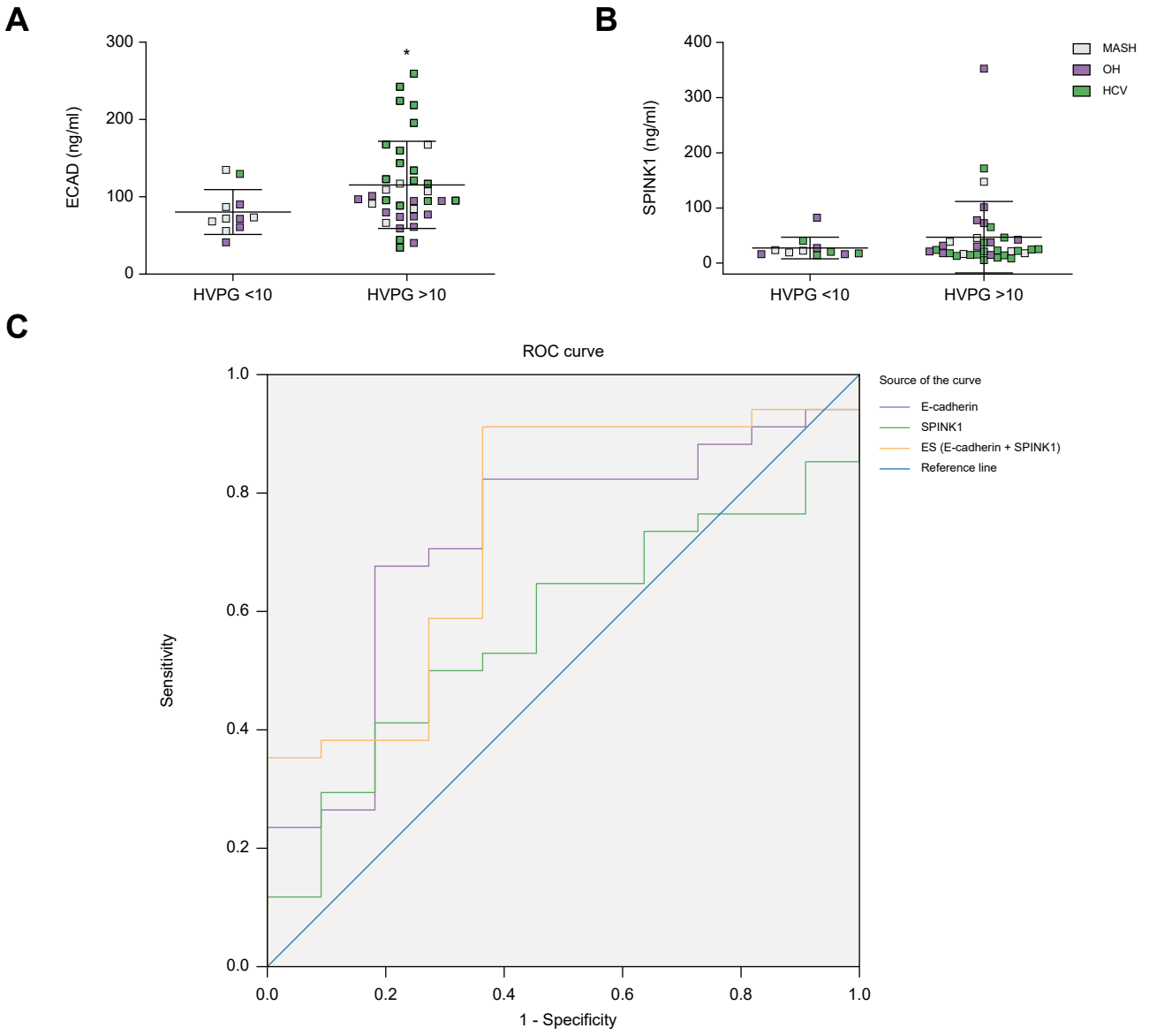

D

Marker	n (</>10 mmHg)	AUROC (95% CI)	Cut-off	Sens (%)	Spec (%)	PPV (%)	NPV (%)
ECAD	11/36	0.725 (0.557 to 0.893)	73.731	83.3	63.6	88.22	53.78
SPINK1	11/35	0.577 (0.401 to 0.752)	20.765	65.7	54.5	82.13	33.31
ECAD + SPINK1	11/35	0.738 (0.564 to 0.911)	0.647	91.4	63.6	88.88	69.92

Fig. 5. Analysis of ECAD, SPINK1, and their combination to predict CSPH. (A) ECAD and (B) SPINK1 in plasma of patients with advanced chronic liver disease with subclinical portal hypertension (HVPG <10; n = 11) or with CSPH (HVPG ≥10; n = 36) of three different aetiologies: MASH, OH, or HCV. (C) ROC curve of ECAD, SPINK1, and ES and (D) its performance. Data were compared using Student's *t* test (**p* <0.05). Values of AUROC, the 95% CI, the cut-off value with better Sens and Spec, PPV, and NPV. AUROC, area under the receiver operating characteristics; CSPH, clinically significant portal hypertension; ECAD, E-cadherin; ES, ECAD + SPINK1; HVPG, hepatic venous pressure gradient; MASH, metabolic-associated steatohepatitis; NPV, negative predictive value; OH, alcohol-associated; PPV, positive predictive value; ROC, receiver operating characteristic; Sens, sensitivity; Spec, specificity; SPINK, serine protease inhibitor Kazal-type 1.

miR-181 regulates CBX7 expression

Given the relevant role of miRNAs as master regulators of gene expression, we used MiRmap tool[24] (University of Geneva, Swiss Institute of Bioinformatics) to identify miRNAs directly interacting with the *CBX7* transcript. Different miRNAs were identified by the software as potential regulators of Cbx7 (Fig. S3A); however, miR-181a-5p (named as miR-181a hereinafter) was identified as an upstream regulator for *CBX7* in both rats and humans and showed the higher predictive score (Fig. S3B). Interestingly, we found that miR-181a expression was significantly upregulated in LSECs isolated from patients with portal hypertension with ACLD and from CCl_4 cirrhotic rats (Fig. 3A).

To study the regulation of miR-181a on *CBX7*, we used an already established *in vitro* model for LSEC capillarisation, consisting of *in vitro* culture of healthy LSECs in plastic Petri dishes to

promote their dedifferentiation.[25,26] To assess the degree of dysfunction of *in vitro* capillarised LSECs, we analysed the expression of landmark markers of functional LSECs, showing a significant reduction in the expression of scavenger receptors *Stab2* (p = 0.004) and *Cd32b* (p <0.001), in addition to a marked decrease in the number of fenestrae, as assessed by scanning electron microscopy (Fig. S4). Remarkably, the de-differentiated LSECs showed a significantly increased miR-181a expression (Fig. 3B; p = 0.015), whereas *CBX7* expression was reduced (Fig. 3C; p <0.0001). To demonstrate the interaction of miR-181a with *CBX7*, we transfected LSECs with a specific miR-181a inhibitor (anti-miR-181a), observing significantly higher levels of *CBX7* mRNA expression (p = 0.021) when miR-181a was inhibited (p = 0.004) (Fig. 3D and E).

CBX7 downstream targets as non-invasive biomarkers of PH

Because CBX7 is a nuclear transcription factor not expected to be found in plasma[27] (Protein Atlas), we wondered whether a non-invasive biomarker for assessing PH/CSPH could be identified using ECAD and SPINK1, two proteins modulated by CBX7 according to previous studies.[28,29]

ECAD and SPINK1 expression was analysed in plasma samples from two independent biomarker cohorts. The discovery biomarker cohort included patients with ACLD from three different aetiologies (HCV, OH, and metabolic-associated CLD) evenly distributed (38.3%, 34%, and 27.7%, respectively) with a mean age of 57 ± 7 years and a mean HVPG of 14.2 ± 5.6 mmHg. Most patients were Child–Pugh A (31 of 47 patients with ACLD). Patient demographics, standard liver function tests, and platelet count are shown in Table S5.

Plasma levels of ECAD (Fig. 4A) and SPINK1 (Fig. 4B) were significantly upregulated (p <0.0001 and p = 0.001, respectively) in patients with PH compared with patients with normal HVPG. AUROC curves to stratify patients between NP and increased portal pressure (Fig. 4C and D) were calculated for both markers alone or combined using the following formula, which was obtained from a binary logistic regression: Y = 1/1 + exp(+4.503 - (0.06*ECAD (ng/ml)) - (0.055*SPINK1 (ng/ml))).

A cut-off value of 0.579 for the combination of ECAD + SPINK1 exhibited the best AUROC (0.911), as compared with AUROC for the individual biomarkers (0.889 for ECAD and 0.747 SPINK1). Test performance statistics for ECAD + SPINK1 showed a 91.3% sensitivity and 83.3% specificity (Fig. 4D).

Regarding CSPH, ECAD expression was significantly upregulated in patients with CSPH (Fig. 5A; p = 0.05), whereas SPINK1 upregulation was not (Fig. 5B; p = 0.32). AUROC curves (Fig. 5C and D) for the performance identifying patients with HVPG below and above 10 mmHg were calculated for both markers and their combination using the following formula: Y = 1/1 + exp(+1.116 - (0.020*ECAD (ng/ml)) - (0.013*SPINK1 (ng/ml)). The combination of ECAD + SPINK1 showed the best predictive power; using a cut-off of 0.647, the test sensitivity was 91.4% and specificity 63.6% (Fig. 5D).

The AUROC of ECAD + SPINK1 was compared and combined with the AUROC of other known markers of liver fibrosis or PH, including transient elastography, alanine aminotransferase (ALT), aspartate aminotransferase (AST), platelet count, the combination of platelets and bilirubin, the combination of transient elastography and platelets, and the FIB-4 and AST to platelet ratio index (APRI) scores (Fig. S5A). These analyses showed that ECAD + SPINK1 has specificity similar to that of previously described markers, but had a higher sensitivity than most, which means that it performs better in detecting those patients who truly have CSPH and is only outperformed by platelets and the combination of platelets and elastography. Importantly, ECAD + SPINK1 improves the overall predictive capacity of other markers when combined (Fig. S5B). ECAD showed a significant correlation with ALT, AST, platelets, and the APRI score, whereas SPINK1 showed no significant correlation with any parameter (Fig. S6).

Finally, we evaluated the predictive capacity of ECAD and SPINK1 in an independent validation cohort of 57 patients with PH and CSPH that also included patients with ACLD from three different aetiologies: 31.6% HCV, 24.6% OH, and 43.8% metabolic-associated CLD, and a mean HVPG of 15 ± 6.9 mmHg. Table S6 shows patient demographics and standard liver function tests. The combination of both biomarkers had an AUROC of 0.941, with a sensitivity of 85.7%, specificity 94.7%, PPV of 96.77%, and NPV 78.16%, at a cut-off value of 0.700.

Discussion

PH is the main factor leading to clinical complications in patients with ACLD, triggering life-threatening manifestations and reducing survival.[1,30] Increased pressure in the portal venous system develops as a consequence of increased resistance to portal blood flow, which in ACLD is determined by microcirculatory dysfunction and structural abnormalities primarily driven by impaired function of sinusoidal cells.[7]

Recent research suggests that cirrhosis-derived mechanobiological signals, such as increased liver stiffness or changes in the matrisome, may, *per se*, represent key stimuli inducing and perpetuating sinusoidal dysfunction and further aggravating the disease in a vicious cycle.[31,32]

Some previous studies have addressed the effects of increased pressure on the vascular endothelium, showing increased proliferation, release of endothelin 1, and cytoskeletal reorganisation with decreased expression of adhesion molecules.[33,34] In the liver field, a recent study described C-X-C motif chemokine ligand 1 upregulation in LSECs exposed to mechanical stretch, inducing a pro-inflammatory niche for neutrophil recruitment and microthrombi formation.[35] Nevertheless, it is important to note that data addressing the effect of pressure in major vessels (within a range of 50–150 mmHg) or biomechanical cyclic stretch might not be the best models to explore LSECs, as these highly specialised endothelial cells are subject to lower pressure and non-pulsatile flow.[36] In the present study, we specifically investigate the impact of hydrodynamic pressure in primary LSECs using a physiologically relevant experimental approach.

Our findings demonstrate for the first time that the deleterious effect of increased pressure on LSECs is defined by a multifaceted deregulation in their phenotype and function, showing modifications in pathways involved in hepatic fibrosis, vasodilatation, or inflammation, thus revealing the significant contribution of increased hydrodynamic pressure in LSEC dysfunction.

Transcriptomic analysis allowed us to identify *CBX7* as an LSEC-specific pressure-sensitive transcription factor in humans, which has not been previously described. CBX7 is a member of the canonical polycomb repressive complex 1, an epigenetic regulator of histones that represses the transcription of genes involved in different processes including cell cycle, environmental stress response, cell fate transition, and cell proliferation and differentiatio[37,38] Loss of CBX7 expression has been

correlated with the grade and development of malignancies in several organs,[39–41] including liver cancer[41,42] However, its role in any endothelium or as a pressure-sensitive molecule has never been outlined.

Considering CBX7 cellular functions as a transcription regulator and its central expression in the liver endothelium, we explored its potential as a novel molecular marker of PH. Studies in human liver samples from two independent cohorts of patients with PH with ACLD of diverse aetiologies showed a negative correlation between *CBX7* and HVPG. Moreover, CBX7 was able to accurately stratify patients with ACLD according to the presence and severity of PH. Interestingly, patients with HCV having achieved a sustained virological response 1 year before by treatment with antivirals exhibited lower HVPG than non-treated patients with ACLD, which was associated with normalised *CBX7* levels.

To further understand CBX7 biology in response to hydrodynamic pressure, we explored its upstream regulation. miR-181a was identified as a specific regulator of *CBX7* using miRmap tool.[24] We found three different target sites in the *CBX7* mRNA for miR-181a-5p regulation in both rats and humans. Shear stress has already been reported to modulate the expression of specific miRNAs in endothelial cells,[43,44] and specifically, miR-181a has been reported to be upregulated in endothelial cells of the aortic valve in response to increased blood flow.[45] Nevertheless, we herein report for the first time that this miRNA responds to changes in hydrodynamic pressure in LSECs. Furthermore, in our study, miR-181a was also found to be upregulated in murine LSECs in cirrhosis and during *in vitro* capillarisation, which leads to a decrease in *CBX7* gene expression. The interaction between miR-181a and *CBX7* was further confirmed by showing that miR-181a silencing induced an upregulation of *CBX7* levels *in vitro*.

As stated above, HVPG is the standard technique for assessing PH, but despite being the most trustable procedure, it has some limitations because it is an invasive procedure with a non-negligible cost and requires specifically trained personnel.[46] Therefore, the discovery of a non-invasive test for assessing this syndrome is of high interest. Recently, different elastography techniques have been in the spotlight as non-invasive methods for assessing PH and fibrosis.[47] Still, these techniques have limitations that do not apply to serum-based tests that could be measured in a routine hospital laboratory. Because of this, we focused on two CBX7 downstream targets (ECAD and SPINK1) as potential plasma biomarkers to categorise patients with ACLD based on their HVPG.

ECAD is a cell adhesion molecule expressed by different cell types that can be found in the plasma as soluble e-cadherin, resulting from the proteolytic cleavage of the cell surface ECAD and indicating several processes including a disruption in cell–cell interaction and increases in cell migration and proliferation.[48] SPINK1 has been reported to increase in the serum of patients with different cancers[49] and to be linked to the progression of HBV-related diseases.[50] Our results showed that ECAD could be a good indicator (and better than SPINK1) for assessing the presence of both PH and CSPH independently of the aetiology of the ACLD. Moreover, we found that combining ECAD and SPINK1 increased the sensitivity and specificity of the predictive ability of the test, with a better predictive power than each marker alone. ECAD + SPINK1 was able to discriminate patients with normal HVPG from those with PH with a sensitivity of 93.1% and a specificity of 83.3%.

Taking into account that an HVPG ≥10 mmHg signals an increased risk of ACLD-related complications,16 we examined whether the use of this combination of biomarkers can detect patients with CSPH, at high risk of progressing to clinical decompensation, that may deserve initiating treatment with non-selective beta-blockers.[51,52] ECAD + SPINK1 classified patients with or without CSPH with 91.4% sensitivity and 63.6% specificity, which are in the upper range or superior to those of other non-invasive methods reported so far including transient elastography[53,54] or platelet count + bilirubin.[55] Our findings were reinforced in an independent validation cohort, where we obtained a comparable predictive score. In addition, we show that combining the expression of these CBX7-related targets with other parameters (including elastography) increases their predictive value. Therefore, this novel analytical approach, which uses simple tools such as ELISA, could be easily implemented in large studies to assess whether it may avoid HVPG measurement for patient selection for preventive therapy and potentially to assess the effect of therapy. Moreover, an increased HVPG is also an indicator of an increased risk of hepatocellular carcinoma (HCC) development. As loss of CBX7 expression has been also described in HCC,[42] it is likely that measuring plasma biomarkers of CBX7 expression may also have a role in assessing the risk of HCC. Thus, our findings open new avenues for future research deciphering the predictive capacity of the herein described biomarkers for the detection of CSPH and HCC in patients with ACLD.

We are aware of the limitations of our study; the exact mechanism by which LSECs sense hydrodynamic changes in pressure remains unknown, and forthcoming studies will be necessary to uncover this mechanosensing cue. Pressure-sensitive mechanoreceptor Piezo1[56] or Ca^{+2}-dependent signalling[57] might be implicated in this process. Moreover, to fully consider the proposed novel biomarkers as a proper method to predict CSPH or HCC, further confirmatory studies with larger international populations are needed. However, and considering the results obtained with the different liver-related markers, we believe that a holistic non-invasive characterisation of patients with PH should rely on the analysis of a combination of several markers, including biomarkers of endothelial de-differentiation.

In summary, our study sheds insight into the prominent role that pathologically relevant pressure exerts in the liver sinusoidal endothelium, inducing the dysregulation of endothelial-relevant pathways, with a direct implication of *CBX7* and its upstream regulator miR-181a. Based on these findings, we propose the combination of the plasmatic levels of ECAD and SPINK1, two of CBX7 targets, as non-invasive biomarkers for PH onset and CSPH monitoring in patients with ACLD.

Abbreviations

ACLD, advanced chronic liver disease; ACTB, beta actin; ALT, alanine aminotransferase; APRI, AST to platelet ratio index; AST, aspartate aminotransferase; AUROC, area under the receiver operating characteristics; cBDL, common bile duct ligation; CBX7, chromobox 7; CCl_4, carbon tetrachloride; CD32b, Fc-gamma receptor IIb; CLD, chronic liver disease; CSPH, clinically significant portal hypertension; DEG, differentially expressed genes; ECAD, E-cadherin; GAPDH,

glyceraldehyde-3-phosphate dehydrogenase; HCC, hepatocellular carcinoma; HSC, hepatic stellate cell; HVPG, hepatic venous pressure gradient; KC, Kupffer cell; LSEC, liver sinusoidal endothelial cell; miRNA, micro RNA; NP, normal pressure; NPV, negative predictive value; PH, portal hypertension; PPV, positive predictive value; SPINK1, serine protease inhibitor Kazal-type 1; STAB2, stabilin 2; TAA, thioacetamide.

Financial support
This work was supported by the Instituto de Salud Carlos III (FIS PI20/00220 and DTS22/00010 to J.G-S and PI20/PI20/01302 to AA), co-funded by the European Union and the Generalitat de Catalunya (AGAUR – 2021 SGR 01322 and 2021 PROD 0036). CIBEREHD is funded by Instituto de Salud Carlos III. Funders had no role in study design, data collection and analysis, decision to publish, or preparation of the manuscript. MO-R has an iPFIS fellowship from the Instituto de Salud Carlos III (IFI16/00016). AG-R has a Sara Borrell fellowship from the Instituto de Salud Carlos III (CD22/00097). MM is a recipient of a Río Hortega grant (CM19/00024) from Instituto de Salud Carlos III, Spain.

Conflicts of interest
The authors declare no competing financial interests.

Please refer to the accompanying ICMJE disclosure forms for further details.

Authors' contributions
Conceived the study: JG-S; Designed the research: MO-R, AG-R, JG-S; Performed the experiments: MO-R, AG-R, LA-J, LP, EC, RP, BS; Analysed the data: MO-R, AG-R, JJL; Directed the research: JG-S; Obtained funding: JG-S; Collected samples and analysed clinical data: MM, LT, LO, PO; Wrote the manuscript: MO-R, AG-R, JG-S; Critically revised the manuscript: RV, JB, AA, JCG-P; Edited and reviewed the final manuscript: all authors.

Data availability statement
All data are included in the main manuscript or Supplementary information. Full RNAseq data were deposited with accession number GSE181255.

Acknowledgements
This study was carried out at the Esther Koplowitz Center – IDIBAPS. The fabrication of Exoliver was performed by the platform of Production of Biomaterials and Biomolecules of the ICTS 'NANBIOSIS', more specifically by the U8 Unit of the CIBER in Bioengineering, Biomaterials and Nanomedicine (CIBERBBN) at the IMB-CNM (CSIC). The authors are indebted to former and current laboratory members from the Liver Vascular Biology Research Group and caregivers from the Barcelona Hepatic Hemodynamic Unit at the Hospital Clinic for their skilled technical assistance. We are indebted to the HCB-IDIBAPS and the Hospital Ramon y Cajal Biobanks for sample and data procurement.

Supplementary data
Supplementary data to this article can be found online at https://doi.org/10.1016/j.jhepr.2023.100722.

References
Author names in bold designate shared co-first authorship.

[1] **Asrani SK**, **Devarbhavi H**, Eaton J, Kamath PS. Burden of liver diseases in the world. J Hepatol 2019;70:151–171.
[2] Jepsen P, Younossi ZM. The global burden of cirrhosis: a review of disability-adjusted life-years lost and unmet needs. J Hepatol 2021;75:S3–S13.
[3] Tsochatzis EA, Bosch J, Burroughs AK. Liver cirrhosis. Lancet 2014;3383:1749–1761.
[4] García-Pagán JC, Gracia-Sancho J, Bosch J. Functional aspects on the pathophysiology of portal hypertension in cirrhosis. J Hepatol 2012;57:458–461.
[5] Gustot T, Stadlbauer V, Laleman W, Alessandria C, Thursz M. Transition to decompensation and acute-on-chronic liver failure: role of predisposing factors and precipitating events. J Hepatol 2021;75:S36–S48.
[6] Ferstl P, Trebicka J. Acute decompensation and acute-on-chronic liver failure. Clin Liver Dis 2021;25:419–430.
[7] Gracia-Sancho J, Marrone G, Fernández-Iglesias A. Hepatic microcirculation and mechanisms of portal hypertension. Nat Rev Gastroenterol Hepatol 2019;16:221–234.
[8] DeLeve LD. Liver sinusoidal endothelial cells in hepatic fibrosis. Hepatology 2015;61:1740–1746.
[9] **Gracia-Sancho J**, **Caparrós E**, **Fernández-Iglesias A**, **Francés R**. Role of liver sinusoidal endothelial cells in liver diseases. Nat Rev Gastroenterol Hepatol 2021;18:411–431.
[10] Babbs C, Haboubi NY, Mellor JM, Smith A, Rowan BP, Warnes TW. Endothelial cell transformation in primary biliary cirrhosis: a morphological and biochemical study. Hepatology 1990;11:723–729.
[11] Cheluvappa R, Denning GM, Lau GW, Grimm MC, Hilmer SN, Le Couteur DG. Pathogenesis of the hyperlipidemia of Gram-negative bacterial sepsis may involve pathomorphological changes in liver sinusoidal endothelial cells. Int J Infect Dis 2010;14:e857–e867.
[12] Fernández-Iglesias A, Gracia-Sancho J. How to face chronic liver disease: the sinusoidal perspective. Front Med 2017;4:7.
[13] Marrone G, Shah VH, Gracia-Sancho J. Sinusoidal communication in liver fibrosis and regeneration. J Hepatol 2016;65:608–617.
[14] Ripoll C, Groszmann R, Garcia-Tsao G, Grace N, Burroughs A, Planas R, et al. Hepatic venous pressure gradient predicts clinical decompensation in patients with compensated cirrhosis. Gastroenterology 2007;133:481–488.
[15] Bosch J, Iwakiri Y. The portal hypertension syndrome: etiology, classification, relevance, and animal models. Hepatol Int 2018;12(Suppl. 1):1–10.
[16] Bosch J, Abraldes JG, Berzigotti A, García-Pagan JC. The clinical use of HVPG measurements in chronic liver disease. Nat Rev Gastroenterol Hepatol 2009;6:573–582.
[17] **Qi X**, **Berzigotti A**, Cardenas A, Sarin SK. Emerging non-invasive approaches for diagnosis and monitoring of portal hypertension. Lancet Gastroenterol Hepatol 2018;3:708–719.
[18] Procopet B, Berzigotti A. Diagnosis of cirrhosis and portal hypertension: imaging, non-invasive markers of fibrosis and liver biopsy. Gastroenterol Rep 2017;5:79–89.
[19] **Boyer-Diaz Z**, **Aristu-Zabalza P**, Andrés-Rozas M, Robert C, Ortega-Ribera M, Fernández-Iglesias A, et al. Pan-PPAR agonist lanifibranor improves portal hypertension and hepatic fibrosis in experimental advanced chronic liver disease. J Hepatol 2021;74:1188–1199.
[20] **Fernández-Iglesias A**, **Ortega-Ribera M**, Guixé-Muntet S, Gracia-Sancho J. 4 in 1: antibody-free protocol for isolating the main hepatic cells from healthy and cirrhotic single rat livers. J Cel Mol Med 2019;23:877–886.
[21] Ortega-Ribera M, Fernández-Iglesias A, Illa X, Moya A, Molina V, Maeso-Díaz R, et al. Resemblance of the human liver sinusoid in a fluidic device with biomedical and pharmaceutical applications. Biotechnol Bioeng 2018;115:2585–2594.
[22] **Manicardi N**, **Fernández-Iglesias A**, Abad-Jordà L, Royo F, Azkargorta M, Ortega-Ribera M, et al. Transcriptomic profiling of the liver sinusoidal endothelium during cirrhosis reveals stage-specific secretory signature. Cancers 2021;13:2688.
[23] Bosch J, Berzigotti A, Garcia-Pagan JC, Abraldes JG. The management of portal hypertension: rational basis, available treatments and future options. J Hepatol 2008;48(Suppl. 1):68–92.
[24] Vejnar CE, Zdobnov EM. miRmap: comprehensive prediction of microRNA target repression strength. Nucleic Acids Res 2012;40:11673–11683.
[25] Xie G, Choi SS, Syn WK, Michelotti GA, Swiderska M, Karaca G, et al. Hedgehog signalling regulates liver sinusoidal endothelial cell capillarisation. Gut 2013;62:299–309.
[26] DeLeve LD, Wang X, Hu L, Mccuskey MK, McCuskey RS. Rat liver sinusoidal endothelial cell phenotype is maintained by paracrine and autocrine regulation. Am J Physiol Gastrointest Liver Physiol 2004;287:G757–G763.
[27] Uhlén M, Karlsson MJ, Hober A, Svensson AS, Scheffel J, Kotol D, et al. The human secretome. Sci Signal 2019;12:eaaz0274.
[28] Pallante P, Forzati F, Federico A, Arra C, Fusco A. Polycomb protein family member CBX7 plays a critical role in cancer progression. Am J Cancer Res 2015;5:1594–1601.

[29] Pallante P, Sepe R, Federico A, Forzati F, Bianco M, Fusco A. CBX7 modulates the expression of genes critical for cancer progression. PLoS One 2014;9(1–12):e98295.
[30] Younossi ZM, Stepanova M, Younossi Y, Golabi P, Mishra A, Rafiq N, et al. Epidemiology of chronic liver diseases in the USA in the past three decades. Gut 2020;69:564–568.
[31] **Guixé-Muntet S**, **Ortega-Ribera M**, Wang C, Selicean S, Andreu I, Kechagia JZ, et al. Nuclear deformation mediates liver cell mechanosensing in cirrhosis. JHEP Rep 2020;2:100145.
[32] Arteel GE, Naba A. The liver matrisome – looking beyond collagens. JHEP Rep 2020;2:100115.
[33] Ichikawa M, Hiromichi S, Kumagai K, Kumagai H, Ryuzaki M, Nishizawa M, et al. Differential modulation of baroreceptor sensitivity by long-term antihypertensive treatment. Hypertension 1995;26:425–431.
[34] Liu MC, Shih HC, Wu JG, Weng TW, Wu CY, Lu JC, et al. Electrofluidic pressure sensor embedded microfluidic device: a study of endothelial cells under hydrostatic pressure and shear stress combinations. Lab Chip 2013;13:1743–1753.
[35] Hilscher MB, Sehrawat T, Arab JP, Zeng Z, Gao J, Liu M, et al. Mechanical stretch increases expression of CXCL1 in liver sinusoidal endothelial cells to recruit neutrophils, generate sinusoidal microthombi, and promote portal hypertension. Gastroenterology 2019;157:193–209.
[36] Aird WC. Endothelial cell heterogeneity. Cold Spring Harb Perspect Med 2012;2:a006429.
[37] Di Croce L, Helin K. Transcriptional regulation by Polycomb group proteins. Nat Struct Mol Biol 2013;20:1147–1155.
[38] Gil J, O'Loghlen A. PRC1 complex diversity: where is it taking us? Trends Cel Biol 2014;24:632–641.
[39] Pallante P, Federico A, Berlingieri MT, Bianco M, Ferraro A, Forzati F, et al. Loss of the CBX7 gene expression correlates with a highly malignant phenotype in thyroid cancer. Cancer Res 2008;68:6770–6778.
[40] Hinz S, Kempkensteffen C, Christoph F, Krause H, Schrader M, Schostak M, et al. Expression parameters of the polycomb group proteins BMI1, SUZ12, RING1 and CBX7 in urothelial carcinoma of the bladder and their prognostic relevance. Tumour Biol 2008;29:323–329.
[41] Forzati F, Federico A, Pallante P, Abbate A, Esposito F, Malapelle U, et al. CBX7 is a tumor suppressor in mice and humans. J Clin Invest 2012;122:612–623.
[42] **Zhu X**, **Qin M**, Li C, Zeng W, Bei C, Tan C, et al. Downregulated expression of chromobox homolog 7 in hepatocellular carcinoma. Genet Test Mol Biomarkers 2019;23:348–352.
[43] **Kumar S**, **Kim CW**, Simmons RD, Jo H. Role of flow-sensitive microRNAs in endothelial dysfunction and atherosclerosis: mechanosensitive atheromiRs. Arterioscler Thromb Vasc Biol 2014;34:2206–2216.
[44] Holliday CJ, Ankeny RF, Jo H, Nerem RM. Discovery of shear-and side-specific mRNAs and miRNAs in human aortic valvular endothelial cells. Am J Physiol Hear Circ Physiol 2011;301:856–867.
[45] Rathan S, Ankeny CJ, Arjunon S, Ferdous Z, Kumar S, Fernandez Esmerats J, et al. Identification of side- and shear-dependent microRNAs regulating porcine aortic valve pathogenesis. Sci Rep 2016;6:25397.
[46] Vuille-Lessard É, Rodrigues SG, Berzigotti A. Noninvasive detection of clinically significant portal hypertension in compensated advanced chronic liver disease. Clin Liver Dis 2021;25:253–289.
[47] Nicoară-Farcău O, Rusu I, Stefănescu H, Tanțău M, Ion Badea R, Procopeț B. Diagnostic challenges in non-cirrhotic portal hypertension – porto sinusoidal vascular disease. World J Gastroenterol 2020;26:3000–3011.
[48] Grabowska MM, Day ML. Soluble E-cadherin: more than a symptom of disease. Front Biosci 2012;17:1948–1964.
[49] Räsänen K, Itkonen O, Koistinen H, Stenman UH. Emerging roles of SPINK1 in cancer. Clin Chem 2016;62:449–457.
[50] Zhu C, Han H, Li J, Xu L, Liu F, Wu K, et al. Hepatitis B virus X protein-induced serine protease inhibitor kazal type 1 is associated with the progression of HBV-related diseases. Biomed Res Int 2019;2019:9321494.
[51] **Villanueva C**, Albillos A, Genescà J, Garcia-Pagan JC, Calleja JL, Aracil C, et al. β blockers to prevent decompensation of cirrhosis in patients with clinically significant portal hypertension (PREDESCI): a randomised, double-blind, placebo-controlled, multicentre trial. Lancet 2019;393:1597–1608.
[52] de Franchis R, Bosch J, Garcia-Tsao G, Reiberger T, Ripoll C, Abraldes JG, et al. Baveno VII – renewing consensus in portal hypertension. J Hepatol 2022;76:959–974.
[53] Pons M, Augustin S, Scheiner B, Guillaume M, Rosselli M, Rodrigues SG, et al. Noninvasive diagnosis of portal hypertension in patients with compensated advanced chronic liver disease. Am J Gastroenterol 2021;116:723–732.
[54] Grgurevic I, Madir A, Trkulja V, Bozin T, Aralica G, Podrug K, et al. Assessment of clinically significant portal hypertension by two-dimensional shear wave elastography. Eur J Clin Invest 2022;52:e13750.
[55] Park SH, Park TE, Kim YM, Kim SJ, Baik GH, Kim JB, et al. Non-invasive model predicting clinically-significant portal hypertension in patients with advanced fibrosis. J Gastroenterol Hepatol 2009;24:1289–1293.
[56] **Friedrich EE**, Hong Z, **Xiong S**, Zhong M, Di A, Rehman J, et al. Endothelial cell Piezo1 mediates pressure-induced lung vascular hyperpermeability via disruption of adherens junctions. Proc Natl Acad Sci USA 2019;116:12980–12985.
[57] **Wilson C**, **Saunter CD**, Girkin JM, Mccarron JG. Pressure-dependent regulation of Ca2+ signalling in the vascular endothelium. J Physiol 2015;593:5231–5253.